Journal of Alloys and Compounds 504 (2010) L28–L30

Contents lists available at ScienceDirect

Journal of Alloys and Compounds

journal homepage: www.elsevier.com/locate/jallcom

Letter

Acoustic emission from deformed Mg–Y–Nd alloy and this alloy reinforced with SiC particles

Z. Trojanová[a,*], Z. Száraz[b], F. Chmelík[a], P. Lukáč[a]

[a] Department of Physics of Materials, Faculty of Mathematics and Physics, Charles University, Ke Karlovu 5, 121 16 Prague 2, Czech Republic
[b] Institute for Energy, Joint Research Centre, European Commission, P.O. Box 2, 1755ZG Petten, The Netherlands

ARTICLE INFO

Article history:
Received 9 March 2010
Received in revised form 25 May 2010
Accepted 28 May 2010
Available online 9 June 2010

Keywords:
Magnesium alloy
Particulate reinforced composite
Plastic deformation
Acoustic emission
Twinning

ABSTRACT

Mg–5Y–4Nd alloy and Mg–5Y–4Nd/SiC metal matrix composite were deformed at ambient temperature. Acoustic emission (AE) was measured during deformation. The time dependence of the count rate was measured with the two levels of discrimination. Pronounced maximum was observed at the onset of plastic deformation. It was ascribed to massive twinning and glide of dislocations in the alloy. In the composite, the AE activity was lower in comparison with the alloy and two acoustic emission peaks were detected.

1. Introduction

High-strength and creep-resistant Mg–Y–RE alloys, where RE represents rare earth elements (mainly Nd), have recently been developed for the automotive and aerospace industries [1,2]. Among them, the precipitation strengthened WE43 and WE54 alloys [3–5] are very promising due to their excellent mechanical properties. Considerable improvement of mechanical properties can be also achieved through reinforcing with ceramic particles [6]. The incorporation of particles causes a substantial increase of strength and stiffness as well as the creep resistance and wear resistance. Silicon carbide (SiC) particulates are the most preferred reinforcements primarily because enhanced properties can be easily achieved with little or no penalty on the low density of magnesium alloys [7]. Presence of discontinuous particles in a magnesium alloy matrix tends to alter microstructure of the alloy, and mechanical and physical properties [8].

Acoustic emission stems from transient elastic waves which are generated within the material during deformation due to sudden localized and irreversible structure changes like dislocation glide and twinning, which are the main deformation mechanisms in Mg and its alloys due to their hexagonal crystal structure. Thus AE parameters can be used as a measure for the dynamic processes that play a role during plastic deformation of magnesium alloys [9–12].

The objective of the present paper is to characterize plastic deformation of the WE54 magnesium alloy and its composite reinforced with SiC particles using in situ AE measurements and to estimate possible deformation mechanisms in both materials.

2. Experimental

The WE54 alloy (nominal composition: 5 wt.%Y, 4 wt.%Nd, balance Mg) was prepared by the gravity casting. Microstructure of the alloy is introduced in Fig. 1a. The grain sizes were estimated via image analysis using the special software (Lucie). Equiaxial grains had a size of 48 μm. The WE54 alloy reinforced by SiC particles with a volume fraction of 13% was processed by a powder metallurgy method. Gas atomised alloy powder and SiC particles were mixed in an asymmetrically moved mixer with subsequent milling in a ball mill. In order to obtain an optimum dispersion of reinforcement in the matrix it is necessary to assure a certain particle/matrix powder size ratio. The maximum powder size was fixed at 63 μm. The powder was encapsulated in magnesium containers and extruded at 400 °C using a 400 t horizontal extrusion press [13]. The composite samples were not thermally treated. Microstructure of the as prepared composite is shown in Fig. 1b (the micrograph was taken perpendicularly to the extrusion direction). SiC particles are non-uniformly distributed in the matrix; they form in many cases small clusters. The size of sharp bounded more or less uniaxial particles was approximately 9 μm and the grain size in the matrix about 3–4 μm. Light micrographs and scanning electron micrographs showed no pores in the composite and the binding between SiC particles and the matrix was perfect. No defects were found in the vicinity of SiC particles and no chemical reaction at the interface matrix/SiC particles was observed.

Cylindrical samples with the radius of 10 and 15 mm in the length were deformed in an Instron 1186 testing machine at a constant crosshead speed giving an initial strain rate of $2.5 \times 10^{-5}\ s^{-1}$. Deformation experiments were performed at ambient temperature. The computer controlled DAKEL-XEDO-3 AE system was used

* Corresponding author. Tel.: +420 22191458; fax: +420 221911490.
E-mail addresses: ztrojan@met.mff.cuni.cz (Z. Trojanová), zoltan.szaraz@ec.europa.eu (Z. Száraz), chmelik@met.mff.cuni.cz (F. Chmelík), lukac@met.mff.cuni.cz (P. Lukáč).

0925-8388/$ – see front matter
doi:10.1016/j.jallcom.2010.05.138

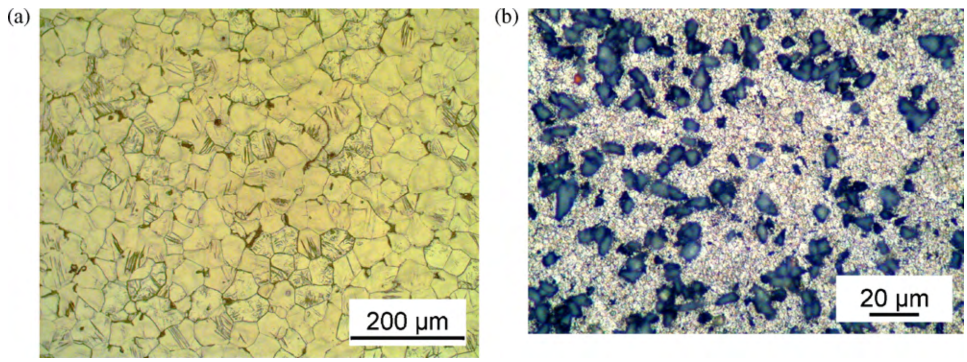

Fig. 1. Microstructure of the undeformed WE54 alloy (a) and WE54/SiC composite (b).

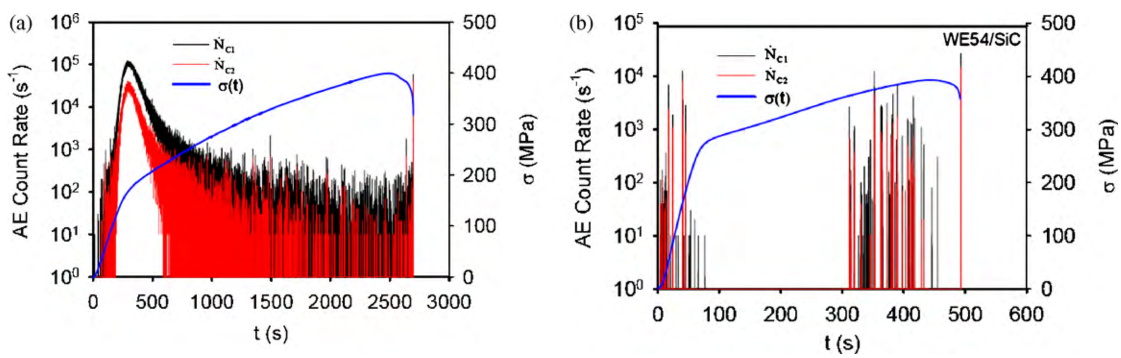

Fig. 2. Deformation curve and AE count rate for the alloy (a) and composite (b) obtained at ambient temperature.

to monitor AE on the basis of two-threshold-level detection, which yields a comprehensive set of AE parameters involving count rates $\dot{N}_{C1}$ and $\dot{N}_{C2}$ (count number per second) at two-threshold levels [14] (giving total AE count and burst AE count by proper setting – see below). The burst AE occurs mainly as a consequence of an instable fashion of plastic deformation (e.g. twinning) or degradation of materials. A miniaturized MST8S piezoelectric transducer (diameter 3 mm, almost point AE detection, a flat response in a frequency band from 100 to 600 kHz, sensitivity 55 dB ref. 1 V_{ef}) was attached on the specimen surface with the help of silicon grease and a spring. The total gain was 90 dB. The AE signal sampling rate was 4 MHz, the threshold voltages for the total AE count $\dot{N}_{C1}$ (level 1) and for the burst AE count $\dot{N}_{C2}$ (level 2) were 730 and 1450 mV, respectively. The full scale of the A/D converter was ±2.4 V.

3. Results and discussion

The engineering stress-time plots together with the time variation of the AE count rates are shown in Fig. 2a. The activity at the onset of deformation up to ∼10–50 s is caused by the fitting of the sample into the clamps of the machine. It is very weak and the counts appeared at the lower threshold level. Counts on both lower and higher level started at 80–100 s. It is possible to identify these counts with the beginning of the twins formation and massive multiplication of dislocations.

The maximum of the AE signal is observed in the vicinity of the yield stress, subsequently the signal activity decreases. The same experiment was performed on the WE54/SiC composite sample. The observed character of the AE activity is different (see Fig. 2b). The AE signal was recorded at the onset of deformation then the AE activity decreased to zero. New AE events were found at higher steps of deformation.

The characteristic maximum of the AE signal observed during plastic deformation of the alloy is caused by the stochastic $\{10\bar{1}2\}\langle10\bar{1}0\rangle$ primary twin formation in the grains unfavourably oriented for the basal slip during the very early stage of plastic deformation. These twins reorient the original lattice on 86.3° and the subsequent straining may continue by the basal slip and secondary twinning. The observed decrease of the AE signal activity is due to the fact that the gliding dislocations and/or secondary twins (under condition of strain hardening) generate lower AE in comparison with the primary twinning [11]. The light micro-

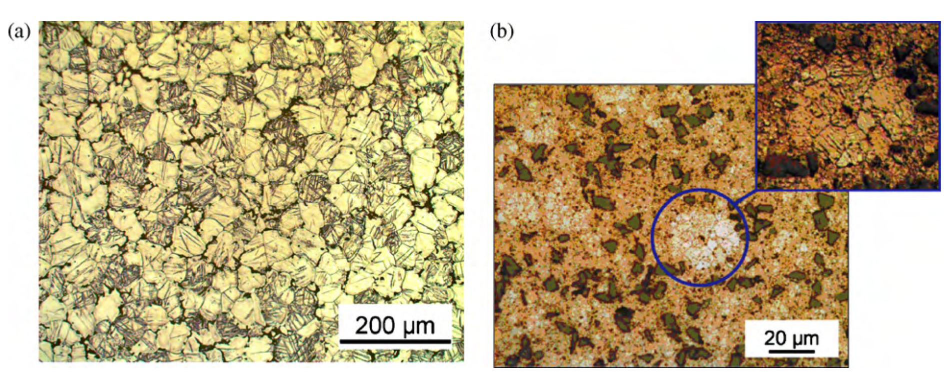

Fig. 3. Light micrographs showing new twins formed during plastic deformation in the alloy (a) and composite (b).

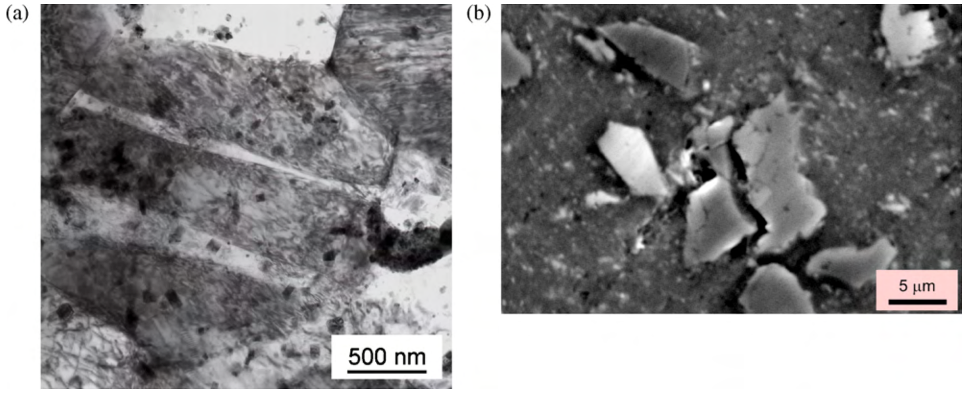

Fig. 4. (a) Transmission electron micrographs showing small twins in the grain. (b) Scanning electron micrograph showing broken particles on the surface of the deformed sample. Decohesion between the matrix and particles is also visible.

graphs revealed high density of newly created twins. Twinning may reorient the basal planes so that they become more favourably oriented for slip [15].

As noted above, the AE signal measured during plastic deformation of WE54/SiC composite has different character in comparison to the alloy. No intense AE signal was found. While the AE signal from the alloy reached 10^5 counts/s at its maximum, in the composite only separated AE events with the count rate of 10^4/s were observed. The observed AE maximum at the onset of plastic deformation is connected with the yield point ($\sigma_{02} \cong 280$ MPa). Some new twins were observed in the deformed microstructure (Fig. 3b). Slim twins were observed also by the TEM as demonstrated in Fig. 4a. Possible dislocation contribution to the AE signal is very probably marginal due to small grain size. The slip length of dislocations is very short (see dislocation tangles in the left bottom corner of the micrograph Fig. 4a) and therefore the probability of pile ups formation is also very low. The mobility of dislocations is further limited due to presence of small cuboidal particles visible in Fig. 4a.

The AE signal detected at the time point of ∼310 s and onwards is discontinuous, and its sources may be ascribed to damage processes. Specifically, with the addition of the reinforcing phase, the geometrically necessary dislocations are generated to accommodate the plastic mismatch in the matrix. The stress concentrations in the vicinity of reinforcing SiC particles may achieve their critical value and a breakage of particles and/or a release of cracks (decohesion) between the matrix and particles can occur. Both processes are considered as strong sources of the AE signal [16]. The broken SiC particles and also cracks in the vicinity of particles were observed at the polished surface of the sample deformed to failure (see Fig. 4b).

These mechanisms are very probably the reason for the observed AE maximum, detected at higher strains. Mummery et al. [17] studied AE during deformation of aluminium based composites reinforced with SiC particles. They focussed their attention on the influence of the particle size and volume fraction on the AE activity and strengthening. They used composites with the particle size of 3, 10 a 30 μm and with the particle volume fraction of 5%, 10% a 20%, respectively. Two main mechanisms were detected during plastic deformation: breakage of particles and decohesion in the particle–matrix interface. They estimated an increase in the AE activity with increasing particle size and increasing volume fraction of the reinforcing phase. Based on these results we may consider localization of the plastic deformation and fracture of the sample if the number of broken particles achieves its critical value.

4. Conclusions

Magnesium alloy WE54 and this alloy reinforced with SiC particles were deformed at ambient temperature with in situ measurements of acoustic emission activity. A pronounced maximum of the AE activity observed at the beginning of plastic deformation of the alloy was ascribed to twinning and dislocation glide. The AE signal detected during plastic deformation of the WE54/SiC composite is weaker. This difference is caused by smaller grains in the composite. The first maximum at the onset of plastic deformation may be ascribed to twinning and dislocation glide while the second maximum estimated at a higher strain is caused by the breakage of particles and decohesion between particles and the matrix. Monitoring of the acoustic emission signal in particulate reinforced magnesium alloy revealed to be an appropriate method for accurate investigations on deformation mechanisms and reinforcement damage during loading.

Acknowledgements

The authors thank the Czech Science Foundation for financial support under grant 106/07/1393.

References

[1] I.J. Polmear, Mater. Sci. Technol. 10 (1994) 1–16.
[2] P.J. Apps, H. Karimzadeh, J.F. King, G.W. Lorimer, Scripta Mater. 48 (2003) 1023–1028.
[3] J.F. Nie, B. Muddle, Scripta Mater. 40 (1999) 1089–1094.
[4] J.F. Nie, Scripta Mater. 48 (2003) 1009–1015.
[5] H. Beladi, M.R. Barnett, Mater. Sci. Eng. A 452–453 (2007) 306–312.
[6] Z. Száraz, Z. Trojanová, M. Cabbibo, E. Evangelista, Mater. Sci. Eng. A 462 (2007) 225–229.
[7] S. Seshan, J. Jayamathy, S.V. Kailas, T.S. Srivatsan, Mater. Sci. Eng. A 363 (2003) 345–351.
[8] J. Jayamathy, S.V. Kailas, K. Kumar, S. Seshan, T.S. Srivatsan, Mater. Sci. Eng. A 393 (2005) 27–35.
[9] C.R. Heiple, S.H. Carpenter, J. Acoust. Emission 6 (1987) 177–204, 215-237.
[10] K. Máthis, F. Chmelík, M. Janeček, B. Hadzima, Z. Trojanová, P. Lukáč, Acta Mater. 54 (2006) 5361–5366.
[11] K. Máthis, F. Chmelík, Z. Trojanová, P. Lukáč, J. Lendvai, Mater. Sci. Eng. A 387–389 (2004) 331–335.
[12] P. Dobroň, J. Bohlen, F. Chmelík, P. Lukáč, D. Letzig, K.U. Kainer, Mater. Sci. Eng. A 462 (2007) 307–310.
[13] J. Schröder, K.U. Kainer, B.L. Mordike, In: L. Mordike, F. Hehmann (Eds.), Magnesium Alloys and Their Applications, B, (1992), pp. 469–478.
[14] Standard Practice for Acoustic Emission Examination of Fiberglass Reinforced Plastic Resin, ASTM E 1067-85, Tank/Vessels, May 31, 1985.
[15] J.W. Christian, S. Mahajan, Prog. Mater. Sci. 39 (1995) 1–157.
[16] K. Ono, Proceedings of the Second Acoustic Emission Symposium, Jpn. Ind. Planning Assoc. Tokyo, Sec. 4, Tokyo, Japan, 1974, p. 1.
[17] P.M. Mummery, B. Derby, C.B. Scruby, Acta Metall. Mater. 41 (1993) 1431–1445.